View metadata, citation and similar papers at core.ac.uk

brought to you by CORE

provided by College of William & Mary: W&M Publish

W&M ScholarWorks

VIMS Articles

2013

Linking dynamics of transport timescale and variations of hypoxia in the Chesapeake Bay

Bo Hong
South China University of Technology

Jian Shen
Virginia Institute of Marine Science, shen@vims.edu

Follow this and additional works at: https://scholarworks.wm.edu/vimsarticles

 Part of the Marine Biology Commons

Recommended Citation

Hong, Bo and Shen, Jian, "Linking dynamics of transport timescale and variations of hypoxia in the Chesapeake Bay" (2013). *VIMS Articles*. 254.
https://scholarworks.wm.edu/vimsarticles/254

This Article is brought to you for free and open access by W&M ScholarWorks. It has been accepted for inclusion in VIMS Articles by an authorized administrator of W&M ScholarWorks. For more information, please contact scholarworks@wm.edu.

JOURNAL OF GEOPHYSICAL RESEARCH: OCEANS, VOL. 118, 6017–6029, doi:10.1002/2013JC008859, 2013

Linking dynamics of transport timescale and variations of hypoxia in the Chesapeake Bay

Bo Hong[1] and Jian Shen[2]

Received 15 February 2013; revised 3 October 2013; accepted 15 October 2013; published 13 November 2013.

[1] Dissolved oxygen (DO) replenishment in the bottom waters of an estuary depends on physical processes that are significantly influenced by external forcings. The vertical exchange time (VET) is introduced in this study to quantify the physical processes that regulate the DO replenishment in the Chesapeake Bay. A 3-D numerical model was applied to simulate the circulation, VET, and DO. Results indicate that VET is a suitable parameter for evaluating the bottom DO condition over both seasonal and interannual timescales. The VET is negatively correlated with the bottom DO. Hypoxia (DO <2 mg L^{-1}) will develop in the Bay when VET is greater than 23 days in summer if mean total DO consumption rate is about 0.3 g O_2 m^{-3} d^{-1}. This critical VET value may vary around 23 days when the total DO consumption rate changes. The VET volume (volume of water mass with VET >23 days) can account for 77% of variations of hypoxic volume in the main Bay. The VET cannot explain all the DO variations as it can only account for the contribution of physical processes that regulate DO replenishment. It is found that the short-term vertical exchange process is highly controlled by the wind forcing. The VET volume decreases when the high-speed wind events are frequent. The summertime VET volume is less sensitive to short-term variations (pulses) of river discharge. It is sensitive to the total amount of river discharge and the high VET volume can be expected in the wet year.

Citation: Hong, B., and J. Shen (2013), Linking dynamics of transport timescale and variations of hypoxia in the Chesapeake Bay, *J. Geophys. Res. Oceans*, *118*, 6017–6029, doi:10.1002/2013JC008859.

1. Introduction

[2] Dissolved oxygen (DO) is an important measure of health in estuaries and other coastal systems. The recurring phenomenon of oxygen depletion in bottom waters from late spring to summer has been widely observed in the Chesapeake Bay [e.g., *Hagy et al*., 2004], Long Island Sound [e.g., *Wilson et al*., 2008], Gulf of Mexico [e.g., *Rabalais et al*., 2002], and many other areas. In Chesapeake Bay, hypoxic conditions occur in the central portion of the Bay (102–222 km upstream of the Bay mouth) for most or all of the summer [*Hagy et al*., 2004]. Hypoxia is a routine phenomenon in western Long Island Sound since the mid-1980s and the minimum DO concentration is declining.

[3] As hypoxia can cause significant ecological harm in both estuarine and coastal waters, there are many studies dedicated to investigating the dominant factors that modulate the DO concentration in bottom waters. By analyzing bottom DO and density stratification in western Long Island Sound, *Wilson et al*. [2008] indicated that the wind-induced current shear plays an important role in controlling stratification and vertical mixing. Interannual variations in both the direction and directional constancy of summertime winds over western Long Island Sound are shown to control the ventilation of bottom waters and thereby the seasonal development of hypoxia. Numerical studies of *Scully* [2010a] demonstrated that the interaction between wind-driven lateral circulation and enhanced vertical mixing over shoal regions is the important mechanism for replenishing oxygen to hypoxic subpycnocline waters. The effectiveness of this mechanism is strongly influenced by the direction of wind forcing. On the other hand, studies of *Seliger and Boggs* [1988] revealed the correlation between summertime Chesapeake Bay hypoxia and springtime discharge from the Susquehanna River. Spring river flow is an extremely strong predictor of summer water column stratification in the middle Chesapeake Bay [*Boicourt*, 1992; *Hagy*, 2002], which affects vertical mixing of DO across the pycnocline [*Hagy*, 2002], and is one of several important factors contributing to the formation of hypoxia. The river flow as a predictor of hypoxia encompasses both direct physical effects and indirect biological effects associated with increased nutrient loading during high flow periods [*Hagy et al*., 2004]. By studying the long-term trends of eutrophication in Chesapeake Bay, *Cerco* [1995]

[1]School of Civil and Transportation Engineering, South China University of Technology, Guangzhou, China.
[2]Virginia Institute of Marine Science, College of William and Mary, Gloucester Point, Virginia, USA.

Corresponding author: J. Shen, Virginia Institute of Marine Science, College of William and Mary, Gloucester Point, VA 23062, USA. (shen@vims.edu)

©2013. American Geophysical Union. All Rights Reserved.
2169-9275/13/10.1002/2013JC008859

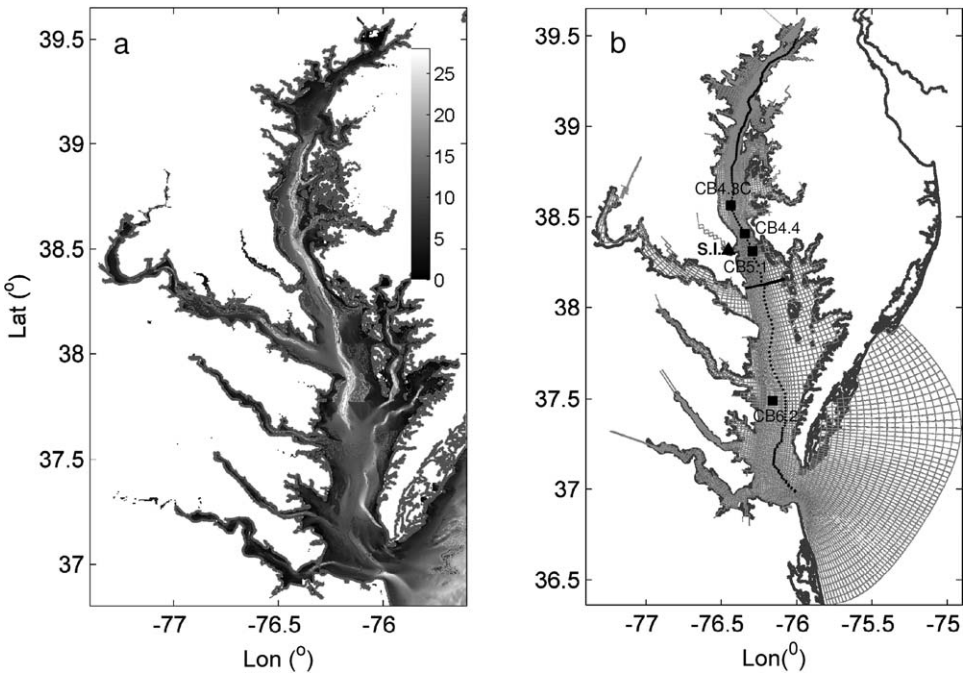

Figure 1. (a) Bathymetry of the Chesapeake Bay; (b) curvilinear orthogonal grid for the Chesapeake Bay model. The selected sections and stations are marked. S.I. represents Solomons Island wind station.

indicated that, over the past 30 years, the maximum variation of anoxic volume attributable to runoff-induced nutrient loading was only 65% of the anoxia caused by high stratification. His results suggested that the hydrodynamic process was one of the major determinants of anoxia variation in the bottom water. In a study of Virginia tributaries of the Chesapeake Bay, *Kuo and Neilson* [1987] linked hypoxia severity to the gravitational circulation. Tributaries with low runoff and weak circulation exhibited more hypoxia than the tributary with the highest runoff and strongest circulation. The residence time of the bottom water is longer when the gravitational circulation is weak. Therefore, water parcels were exposed to bottom-oxygen demand for a longer period. However, in the mainstem of the Bay, the stratification is sufficient to overcome the beneficial effects of strong gravitational circulation and the vertical exchange process is the dominant physical process for modulating the bottom water DO in the middle and upper portions of the Bay mainstem.

[4] Hypoxia occurs when the oxygen consumption by biogeochemical processes exceeds replenishment by physical processes. *Shen et al*. [2013] presented a simplified conceptual model of the relationships between estuarine transport timescales and bottom water DO. The timescales were used in their study to quantify the strength of estuarine circulation, vertical exchange, and the total oxygen consumption rate of biochemical processes. Using transport timescales to quantify the physical oceanographic and biochemical processes has many advantages and has been widely used for inferring the circulation and mixing in estuaries and oceans [*Hohmann et al*., 1998; *Schlosser et al*., 2001; *Shen and Haas*, 2004; *Hong and Shen*, 2012], studying rates of biochemical processes [*Sarmiento et al*., 1990; *Hohmann et al*., 1998; *Lucas et al*., 2009], and estimating ventilation rates of lakes, estuaries, and ocean basins [*England*, 1995; *Jenkins*, 1987; *Gustafsson and Bendtsen*, 2007]. The transport timescale can be calculated as water age and is not directly observable. Transient tracers and isotopes are usually used in numerical models and natural waters to infer water age. In this way, the transport time represents the elapsed time since the water was last in contact with the tracer source [*Deleersnijder et al*., 2001; *Waugh et al*., 2003; *Delhez et al*., 2004].

[5] The Chesapeake Bay is one of the most productive estuaries in the U.S. (Figure 1a). The Susquehanna River contributes 62% of the gauged flow to Chesapeake Bay [*Cerco*, 1995]. Consequently, Susquehanna runoff is a prime determinant of circulation and density stratification in the mainstem of the Bay. Over the last four decades, the volume of hypoxic and anoxic water in the Chesapeake Bay has more than tripled due to excessive nutrient inputs [*Hagy et al*., 2004]. In many years, the hypoxic volume comprises almost a quarter of the water in the mainstem of the Bay during the summer months [*Chesapeake Bay Foundation*, 2008]. On average, DO levels in bottom areas of the Bay begin to decline in March, become hypoxic in May, and do not return to healthy levels until October or November [*Chesapeake Bay Foundation*, 2008]. Quantifying the competition between physical processes and biochemical processes for regulating DO in the bottom waters of an estuary is crucial but remains difficult under realistic situations. In this paper, we applied a 3-D numerical model to reproduce the dynamic circulation and DO variations in the Chesapeake Bay. The transport timescales are calculated to quantify the contributions of different physical processes that regulate the DO replenishment in the Bay. We aim to pursue the correlations between the bottom

water DO and vertical exchange time, which will be used to measure physical processes that regulate the DO replenishment.

[6] The paper is organized as follows. The model configuration is introduced in section 2. The model calibration is shown in section 3. Section 4 presents the results. Section 5 presents the discussion. Conclusions are given in section 6.

2. Methods

2.1. Hydrodynamic Model Description and Configuration

[7] The three-dimensional hydrodynamic-eutrophication model (HEM-3D) developed by the Virginia Institute of Marine Science is used for this study. The hydrodynamic portion of the HEM-3D model is the environmental fluid dynamics code (EFDC). The detailed description of the HEM-3D model can be found in *Hamrick and Wu* [1997]. The model uses curvilinear, orthogonal horizontal coordinates, and sigma vertical coordinates to represent the physical characteristics of a water body. The Mellor and Yamada level 2.5 turbulence closure scheme [*Mellor and Yamada*, 1982; *Galperin et al*., 1988] was implemented in the model. As participants of the NOAA/SURA Estuarine Hydrodynamics and Hypoxia Modeling Testbed, this model had been fully calibrated for tide, salinity, and current velocity against the available observations in the Chesapeake Bay. This model had been successfully applied to the Chesapeake Bay for the sea level rise study [*Hong and Shen*, 2012]. The same model configuration as was used in *Hong and Shen* [2012] (including model grids, open boundary conditions, forcing fields, initial fields, etc.) is used in this study. The model grids and computation domain are shown in Figure 1b.

2.2. Dissolved Oxygen Simulation

[8] A DO model with simplified parameters is coupled with the EFDC model. The DO dynamics are controlled by net DO transport, biogeochemical oxygen consumption, and reaeration. The DO processes can be described as follows:

$$\frac{\partial O}{\partial t}+u\frac{\partial O}{\partial x}+v\frac{\partial O}{\partial y}+w\frac{\partial O}{\partial z}=\frac{\partial}{\partial z}A_v\frac{\partial O}{\partial z}-B_c \tag{1}$$

where O is DO concentration in the water column (mg L^{-1}); u, v, w are the along-Bay, across-Bay, and vertical velocity components (m s^{-1}), respectively; A_v is the eddy diffusivity (m^2 s^{-1}) calculated by the hydrodynamic model; and B_c is the oxygen consumption rate of organic carbon and other processes in the water column (g O_2 m^{-3} d^{-1}). This rate was used to account for the net oxygen lost in the water column. Therefore, no phytoplankton activities are simulated. At the water surface ($z=0$), $A_v\partial O/\partial z=\theta_s$, where θ_s is the surface oxygen flux. At the water-sediment interface ($z=H$), $A_v\partial O/\partial z=\mathrm{SOD}$, where SOD is the sediment oxygen demand (g O_2 m^{-2} d^{-1}). In our simulation, SOD is prescribed as 1.0 g O_2 m^{-2} d^{-1}. This value is slightly higher than the measured high value of 0.86 g O_2 m^{-2} d^{-1} reported by *Cowan and Boynton* [1996], but lower than the value reported by *Boynton and Kemp* [1985]. *Boynton and Kemp* [1985] measured the water column respiration rate in the Bay. Combined with observed SOD, they estimated the total oxygen consumption rates at different stations in May and August ranged from 3.2 to 19.1 g O_2 m^{-2} d^{-1} with a mean value of 7.52. For the subpycnocline thickness of 20 m in the middle Bay, the total oxygen consumption rates ranged from 0.16 to 0.96 g O_2 m^{-3} d^{-1}, with a mean rate of 0.38. A constant water column oxygen consumption rate (B_c) of 0.23 g O_2 m^{-3} d^{-1} at 20°C was used. This rate corrected by a temperature-related function of $1.06^{(T-20)}$ (T is temperature °C) was implemented in the model to account for seasonal variations [*Thomann and Mueller*, 1987]. As T has spatial and temporal variations, the resulting oxygen consumption rate also varies spatially and temporally. The rate will be 0.30 g O_2 m^{-3} d^{-1} at 25°C. The same temperature-related function was also applied to SOD. The open boundary oxygen values were prescribed by the saturation values, which are computed as a function of temperature and salinity [*Park et al*., 1995]. Using a model with sophisticated biochemical processes, such as the Chesapeake Bay Program Model [*Cerco*, 1995], one can simulate nutrient and phytoplankton dynamics and account for DO variations more realistically and accurately. However, the use of this simplified DO model is not for the purpose of predicting the DO based on nutrient input and phytoplankton dynamics, but to capture the DO variations based on lumped biological processes and observed mean parameters, which will allow us to conduct a diagnostic study of the influence of physical processes on DO dynamics [*Scully*, 2010a].

2.3. Transport Timescale Calculation

[9] The transport timescale is calculated as mean water age, which is governed by the following equations:

$$\frac{\partial C(t,x,y,z)}{\partial t}+\nabla(\vec{u}C(t,x,y,z)-K\nabla C(t,x,y,z))=0 \tag{2}$$

$$\frac{\partial \alpha(t,x,y,z)}{\partial t}+\nabla(\vec{u}\alpha(t,x,y,z)-K\nabla \alpha(t,x,y,z))=C(t,x,y,z) \tag{3}$$

[10] The mean water age can be calculated as follows:

$$a(t,x,y,z)=\frac{\alpha(t,x,y,z)}{C(t,x,y,z)} \tag{4}$$

where $\nabla=\vec{i}\frac{\partial}{\partial x}+\vec{j}\frac{\partial}{\partial y}+\vec{k}\frac{\partial}{\partial k}$, $C(t,x,y,z)$ is the tracer concentration, $\alpha(t,x,y,z)$ is age concentration, $\vec{u}$ is the velocity field, and K is the diffusivity tensor. Conservative tracers were used to calculate the transport timescales of the physical processes in the Bay based on equations (2) and (3). For computing the vertical exchange time (VET), tracers are released throughout the entire surface of the Bay. At the surface, the boundary conditions are specified as $C(t,x,y,z)=1$ and $\alpha(t,x,y,z)=0$. At the bottom, the boundary conditions are specified as $\partial C(t,x,y,z)/\partial z=0$ and $\partial\alpha(t,x,y,z)/\partial z=0$ [*Gustafsson and Bendtsen*, 2007]. The vertical exchange time represents the elapsed time since the water was last in contact with the water surface. As the lateral circulation can also transport water parcels from the surface layer (or well-oxygenated regions) to the bottom

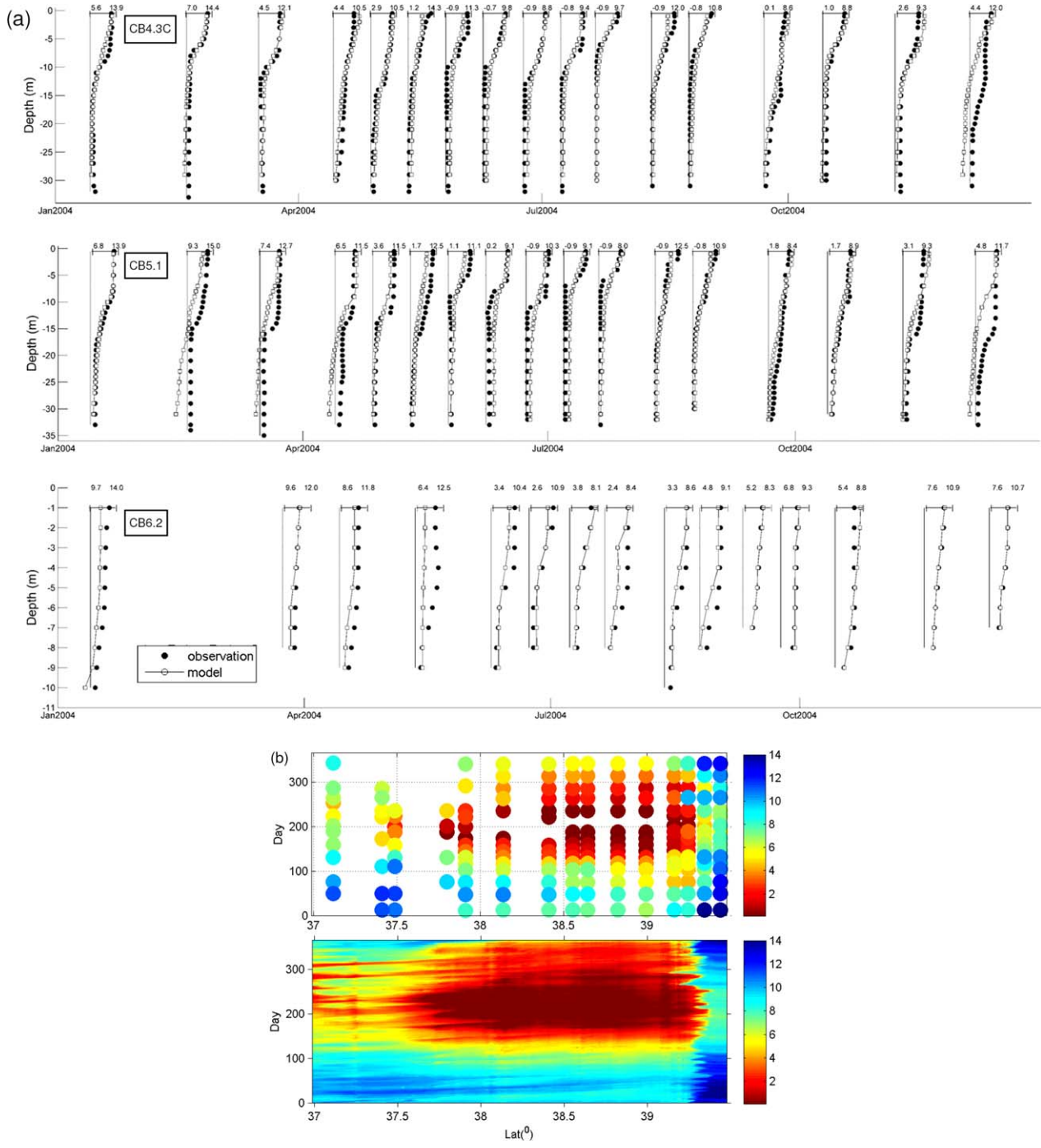

Figure 2. Model-data comparisons of DO in 2004. (a) Vertical profiles at Stations CB4.3C, CB5.1, and CB6.2; (b) temporal variations of (top) observed and (bottom) modeled bottom DO distribution along the main channel of the Bay.

layer where hypoxia is likely to appear, the calculated vertical exchange time not only includes the contribution of vertical mixing, but also includes the contribution of lateral circulation that induces exchange between surface and bottom layers of the Bay. The resulting water age at any location represents the transport time required for the water parcel to be transported from the water surface to that location, regardless of its pathway. A similar calculation had been applied in the Chesapeake Bay [*Hong and Shen*, 2012].

3. Dissolved Oxygen Validation

[11] As the hydrodynamic model had been calibrated and shown in *Hong and Shen* [2012], only the DO model calibration is shown below. The observed results in 2004 are used for the model calibration. The DO data were obtained from the Chesapeake Bay Water Quality Monitoring Program (http://www.chesapeakebay.net/data_waterquality.aspx). Under this program, the water column was sampled at least monthly at several stations throughout the

Bay since 1984. The modeled DO profiles are compared against available observations. Results at selected stations located in the upper (CB4.3C), middle (CB5.1), and lower (CB6.2) portions of the Bay are shown in Figure 2a. The vertical structures together with the seasonal variations that show in the measured DO data can be reproduced by the model simulation. The DO differences between the surface and bottom layers are larger in the middle and upper-Bay than in the lower-Bay. The comparison of bottom DO along the main channel of the Bay is shown in Figure 2b. Both the timing of hypoxia occurrence and DO concentration can be well reproduced by the model. The low DO water (DO <2 mg L^{-1}) mainly occupies the area between latitudes 37.5°N and 39.2°N, which corresponds to the mouths of Rappahannock River and the Baltimore Harbor, respectively. These comparisons provided validation that the model results are reasonable and can be used for the following analyses.

4. Results

4.1. Correlation of Vertical Exchange Time and Bottom DO

[12] Analyses are first conducted along the cross-Bay section that is located in the mid-Bay (marked in Figure 1b). Since the DO depletion mainly occurs in bottom waters, both the DO and the VET are averaged at the cross-Bay section for bottom waters deeper than 8 m. The results are shown in Figure 3a. The averaged VET shows good negative correlation with the averaged DO. The correlation coefficient is -0.81 with a 95% confidence level. In 2004, the hypoxia (DO <2 mg L^{-1}) occurs around Day 155 and lasts through Day 305. The VET profile also has obvious seasonal variations. The larger VET mainly appears in the summer and the water mass with VET >23 days appeared in the bottom layers during the hypoxia period. The scatter diagram of VET and DO along this cross-Bay section is shown in Figure 3b. The linear fit of the summertime data (Day 150–255) gives the relationship equation DO $= 7.5-0.235 \times$ VET. According to this equation, the DO will be less than 2 mg L^{-1} when the VET is greater than 23 days. This linear relationship is based on the data points with VET <30 days because the DO concentrations level out as DO near the bottom is depleted when the VET is larger than 30 days (Figure 3b).

[13] The relationship between VET and bottom DO can be evaluated by a simplified conceptual model [*Shen et al*., 2013]. For a partially mixed estuary, the estuarine circulation can be described by a two-layer model [*Pritchard*, 1952; *Officer*, 1976; *MacCready*, 2004]. Assuming steady state for tidally averaged flow, the lower layer oxygen for a uniform estuary is governed by the following equation [*Kuo and Neilson*, 1987]:

$$u\frac{\mathrm{d}O}{\mathrm{d}x}=\frac{k_z}{H}\frac{(O_s-O)}{d}-B \tag{5}$$

where k_z is the vertical exchange rate (m^2 s^{-1}) between the surface and bottom layers. We use this exchange rate to parameterize the overall exchanges between surface and bottom layers. Such vertical exchange can be caused by lateral circulation and other processes, and is not limited to turbulent mixing. B is the total DO consumption rate including both the water column and SOD. The symbol d is the distance between the center of the upper layer and lower layer, and it can be approximated by the bottom layer thickness H. Let $D=O_s-O$ be the DO deficit and, applying the boundary condition $D=D_0$ at the Bay mouth ($x=0$, x is positive toward the upstream), equation (5) can be solved as:

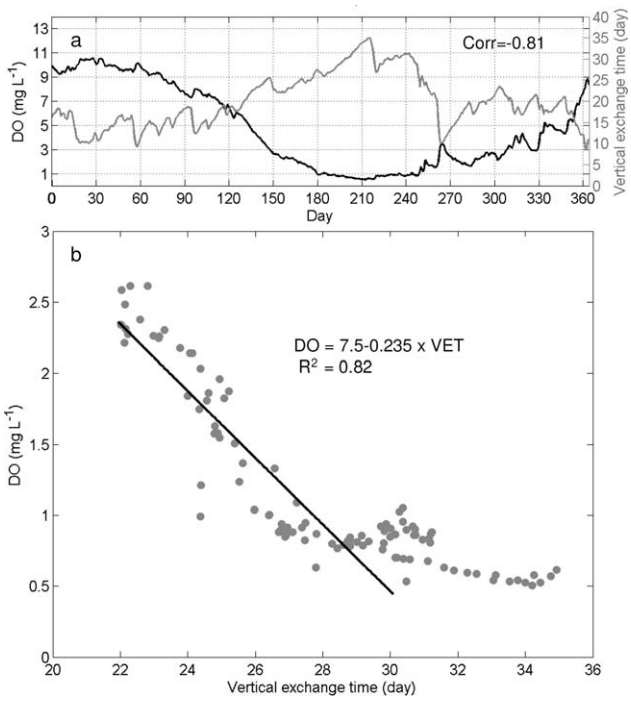

Figure 3. (a) Section-averaged DO and vertical exchange time (VET) along the cross-bay section in the mid-Bay (see Figure 1b for its location). The results are averaged at the cross-bay section for bottom layers with depth >8 m. The correlation coefficient of DO and VET is -0.81 with 95% confidence level; (b) scatter diagram of VET and DO. Solid line is the linear fit: DO $= 7.5-0.235 \times$ VET.

$$\frac{D}{O_s}=\frac{H^2B}{k_zO_s}\left(1-e^{-\frac{k_zx}{H^2u}}\right)+\frac{D_0}{O_s}e^{-\frac{k_zx}{H^2u}},\quad \text{and}\quad D\geq 0 \tag{6}$$

[14] Let $\tau_e=x/u$ be the longitudinal transport timescale that quantifies the travel time of gravitational circulation, $\tau_v=H^2/k_z$ be the vertical exchange timescale that is the time required for the vertical transport of a water parcel between two layers, and $\tau_b=O_s/B$ be the timescale of the biochemical oxygen consumption. We further introduce two dimensionless parameters, τ_b^* and τ_e^*, which are scaled by the vertical exchange timescale as:

$$\tau_b^*=\frac{\tau_b}{\tau_v}\ \text{and}\ \tau_e^*=\frac{\tau_e}{\tau_v} \tag{7}$$

[15] Substituting equation (7) into equation (6) gives:

$$\frac{D}{O_s}=\frac{1}{\tau_b^*}\left(1-e^{-\tau_e^*}\right)+\frac{D_0}{O_s}e^{-\tau_e^*} \tag{8}$$

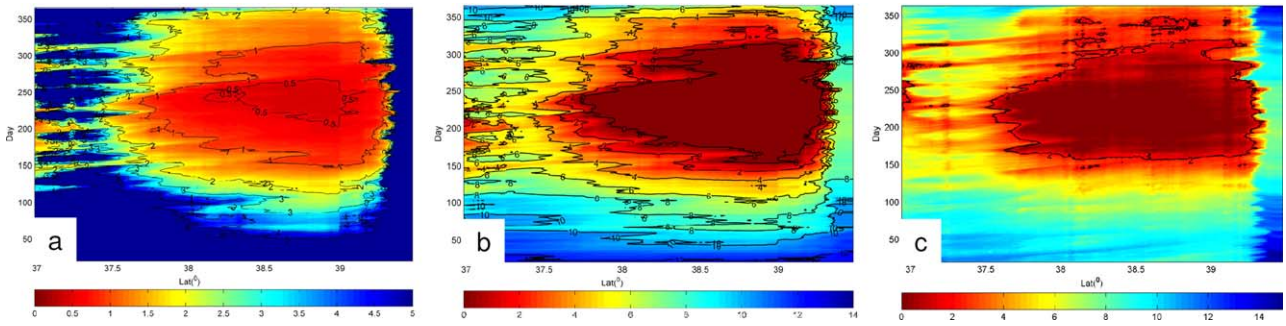

Figure 4. Temporal and spatial profiles along the main channel of the Bay for (a) τ_b/τ_v; (b) bottom DO predicted by the conceptual model; (c) bottom DO simulated by the HEM-3D model. Here, τ_b is the timescale of the biochemical oxygen consumption and τ_v is the vertical exchange timescale.

[16] The term $e^{-\tau_e^*}$ is the effect of gravitational circulation and the second term on the right-hand side of equation (8) accounts for the impact of the open boundary condition, which diminishes as x increases upstream. Here we transform from a function of distance (x) to an equivalent equation (8), which is a function of timescales and gives a Lagrangian perspective of the DO balance equation. For a given DO consumption rate, surface DO, and transport timescale, the bottom DO can be estimated. The longitudinal transport timescale τ_e usually ranges from 100 to 150 days in the mid- to upper-Bay (more than 100 km upstream of the Bay mouth) in summer [*Shen et al*., 2013]. Although the water around the Bay mouth is well oxygenated, the DO within these water parcels will be consumed by the biochemical processes after 100–150 days while they are transported upstream by the gravitational circulation. Therefore, the contribution of gravitational circulation to the mid- and upper-Bay bottom DO replenishment can be neglected. Consequently, the bottom DO replenishment in the mid- to upper-Bay is mainly regulated by the VET and the DO consumption in the water column, which can be expressed as:

$$O = O_s - B \times \tau_v \tag{9}$$

[17] During summer, the saturation DO (O_s) is about 7.1–8.4 mg L^{-1} (T is 21.2–29.0°C) and the total DO consumption rates (B) used for the model simulation range from 0.25 to 0.39 g O_2 m^{-3} d^{-1} with a mean value of about 0.3 g O_2 m^{-3} d^{-1}, which is within the range of observations [*Boynton and Kemp*, 1985]. The result of the linear fit in Figure 3b is consistent with this conceptual model prediction except that the linear fit relationship can only provide constant surface saturation DO (7.5 mg L^{-1}) and DO consumption rate (0.235 g O_2 m^{-3} d^{-1}). The low DO consumption rate obtained from the linear fit is partially due to including data points with VET >28 days as the DO was depleted near the bottom. Based on the conceptual model (equation (9)), the bottom DO ranges from 0.2 to 1.5 mg L^{-1} for a DO consumption rate of 0.3 g O_2 m^{-3} d^{-1}, a VET value of 23 days, and the saturation DO ranges from 7.1 to 8.4 mg L^{-1}.

[18] Using the VET along the main channel of the Bay output by the HEM-3D model, the temporal and spatial distributions of $\tau_b^*(=\tau_b/\tau_v)$ near the bottom along the deep channel of the Bay can be obtained (Figure 4a). By using the nondimensional parameter τ_b^*, DO predicted by equation (8) is shown in Figure 4b. The DO simulated by the HEM-3D model is shown in Figure 4c. It can be seen that the conceptual model predicted results matching our 3-D model-simulated bottom DO in general. It is convincing that the variation of VET is a suitable parameter for evaluating the variation of bottom DO concentration.

4.2. Seasonal Feature of DO and Vertical Transport Time

[19] The seasonally averaged profiles of DO and VET along the main channel of the Bay are presented in Figure 5. In spring (typically represented by March), the mean DO is high throughout the entire water column and the VET is less than 25 days for most of the area (Figures 5a and 5c). The increase of the VET induces a reduction of the bottom DO in summer (Figures 5b and 5d). When bottom DO is only about 14% (1/7) of the surface saturation DO in summer, it will take more than 25 days for the surface saturated DO to be transported by physical processes to the area where DO is less than 2 mg L^{-1}. In summer, the variation of VET around 5–10 m depth is much higher than that in other areas due to the intensified pycnocline. It can be seen that the VET distribution does not match the DO distribution very well because the contributions of biochemical processes cannot be reflected by the VET.

[20] We applied the conceptual model (equation (9)) to estimate DO as a qualitative comparison. Using total DO consumption rates of 0.12 and 0.30 g O_2 m^{-3} d^{-1} (as the springtime and summertime temperatures are around 9 and 25°C, respectively), DO distributions can be estimated based on the averaged VET profile shown in Figures 5c and 5d, respectively. The pattern of estimated along-Bay DO distributions (Figures 5e and 5f) is close to the corresponding results shown in Figures 5a and 5b. These indicate that, by considering temperature and the biochemical processes that are parameterized by the total oxygen consumption rate, DO can be estimated from the VET. The discrepancy can be observed between the results from the conceptual model and the 3-D model, especially around the pycnocline. This is partially due to the fact that conceptual model (equation (9)) only gives the linear relationship that cannot account for the realistic spatial and temporal variations of temperature and DO consumption rates over this 2 month

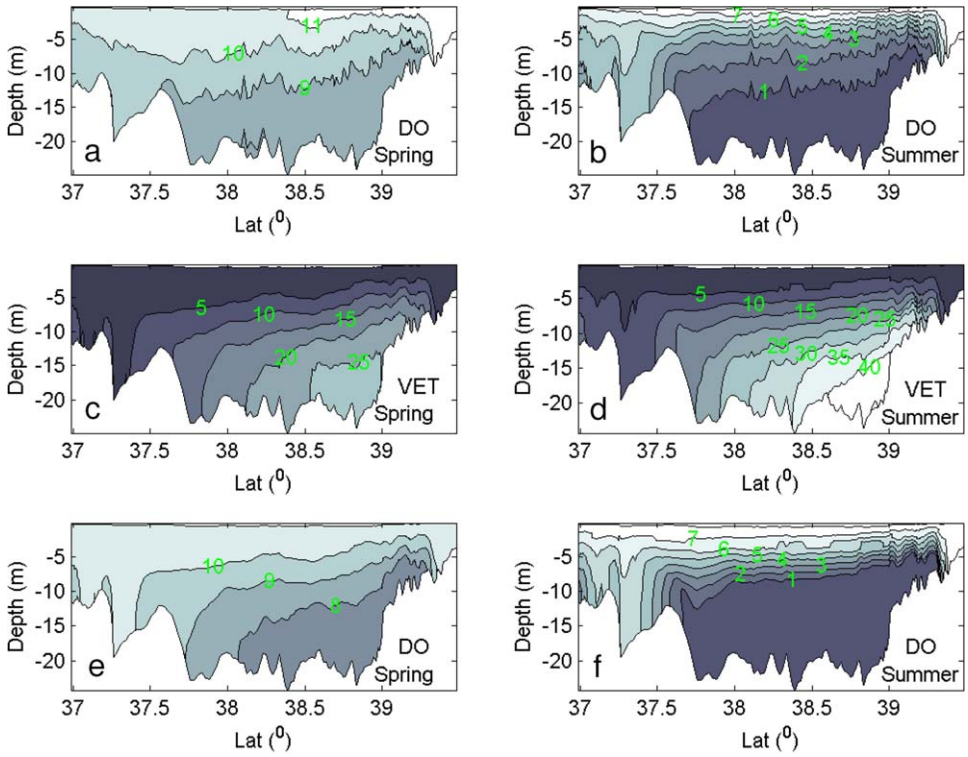

Figure 5. Profiles of (a and b, mg L^{-1}) HEM-3D modeled DO, (c and d, day) vertical exchange time, and (e and f, mg L^{-1}) conceptual model predicted DO along the deep channel of the Bay (the location of this section is marked in Figure 1b). The conceptual model uses vertical exchange time shown in Figures 5c and 5d together with the biochemical DO consumption rate to do the DO prediction. (left) Results are for the typical spring pattern (averaged in March) and (right) results are for the typical summer pattern (averaged from July to August).

period as included in the 3-D model. Besides, the SOD is applied to the bottom boundary layer in the 3-D model. Its influence is not uniformly distributed over the water column and cannot be estimated by a constant DO consumption rate. Although gravitational circulation has a negligible contribution to the mid- and upper-Bay bottom DO replenishment as the DO within the well-oxygenated Bay mouth water will be consumed by the biochemical processes while they are transported to the mid- and upper-Bay, it can transport hypoxic water from the mid-Bay to upstream when hypoxia occurs in the mid-Bay. For example, in 2004, hypoxia was observed in the area south of 38.2°N (see Figure 2b). In the conceptual model, such longitudinal transport of hypoxic water is excluded.

4.3. Effect of Lateral Circulation on Vertical Transport Time and DO

[21] A notable decrease of VET occurred around Day 262 in the mid-Bay region (Figure 3a). It can be seen that such a change of the VET is accompanied by an increase of bottom water DO. We examined the wind forcing and noticed that there is an abrupt change in the wind speed and direction during this period (Figure 6a). *Scully* [2010a] pointed out that the effect of wind-driven lateral circulation is one of the important mechanisms regulating summer DO. The effect of lateral circulation induced DO replenishment during the synoptic event can also be observed through the change of VET. Figures 6b–6e presents the daily averaged DO, VET, lateral circulation, and salinity, respectively, along the cross-Bay section in the mid-Bay from Day 261 to Day 266. Before Day 261, the wind forcing is weak. The strong southeast wind occurs on Day 261. The strong north/northeast wind lasts from Day 262 to the end of Day 264. The strong wind event greatly deepened the upper mixed layer on Days 262 and 263 due to the increased vertical mixing, which can be observed from vertical profiles of DO, VET, and salinity. Meanwhile, the strong counter-clockwise lateral circulation is generated at Day 262 and lasts through Day 266. Study of *Li and Li* [2011] indicated that, under down-estuary winds, a counter-clockwise lateral circulation is generated and steepens isopycnal in the cross-channel sections. The pattern of the lateral circulation in response to the wind events in the present study is consistent with those shown in *Li and Li* [2011]. The strong lateral circulation favored the vertical exchange by transporting water parcels from well-oxygenated regions to stratified regions where hypoxia is likely to appear. Such process greatly reduced the VET and, thereby, enhanced the DO replenishment. The seasonal mean VET in summer is more than 30 days in the deep main channel (Figure 5c). Such a synoptic wind event can greatly shorten the VET and the value of 15 days can be observed in the bottom layer. The salinity profile along this cross-Bay section clearly reflects that the high flow-induced dilution occurs on Day 266 (salinity <10 psu), which is 4 days after the onset of the strong clockwise

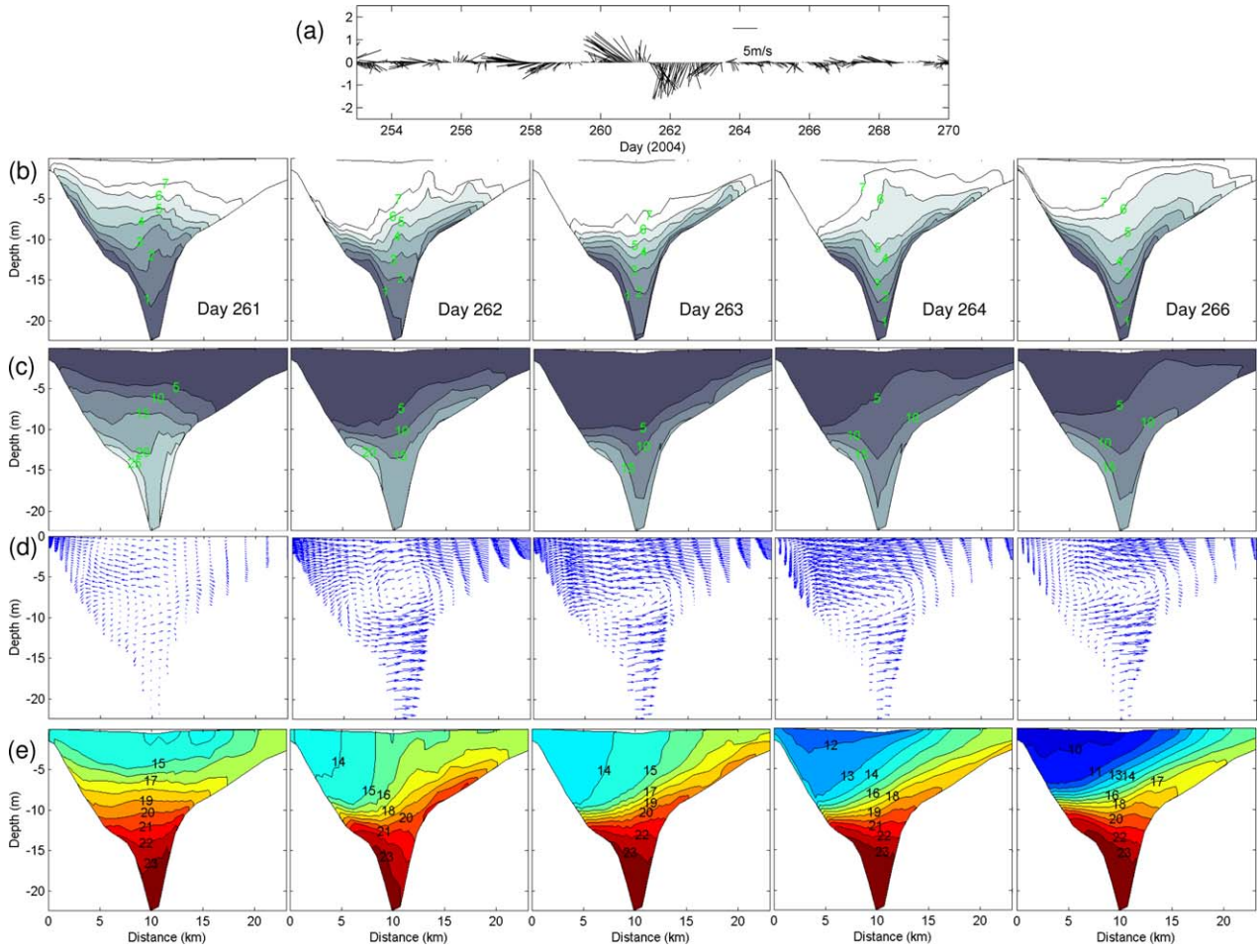

Figure 6. (a) Wind vector observed at Solomons Island station (S.I. marked in Figure 1b); (b–e) daily averaged DO, vertical exchange time, lateral circulation, and salinity for the section across the mid-Bay. From left to right, the presented results are for Day 261–266.

lateral circulation. This information indicates that, during a synoptic event such as a large storm, the wind effect can be immediately observed in the local water column while the effect of high flow is usually delayed. The intensified vertical mixing and lateral circulation greatly reduced the hypoxia volume. The intensified river discharge may facilitate the restoration of stratification. The restored stratification will increase the VET, which will facilitate the following restoration of hypoxic volume. From Figure 3a, such restoration may take about 2 weeks.

5. Discussion

[22] The wind forcing and river discharge are the two major factors that are attributed to the variations of hypoxic volume [e.g., *Hagy et al*., 2004; *Wilson et al.*, 2008; *Scully*, 2010a, 2010b; *Murphy et al*., 2011]. The formation of hypoxia and its extent is regulated by the competition between DO replenishment by physical processes and DO consumption by biochemical processes. While the DO consumption rate is used to parameterize the biochemical processes in our study, we will focus our discussion on the effect of physical processes in replenishing bottom DO.

5.1. Effect of Wind Forcing

[23] The wind-induced vertical mixing and lateral circulation can greatly modify the VET (Figure 6). In order to quantify the wind effect, we conducted two sensitivity experiments: W1 (which doubles the wind speed after Day 150) and W2 (which turns off the wind forcing after Day 150). Other forcings are the same as those in the Base Run (which uses realistic forcing). Day 150 is selected as the starting time for the sensitivity experiments because it is approximately when hypoxia begins in the Bay (see Figure 3a).

[24] The temporal variations of the VET volume (defined as the volume of water mass with vertical exchange time >23 days) are presented in Figure 7a. It can be seen that the VET volume approximates zero when the wind speed is doubled (Run W1). On the contrary, the VET volume is greatly increased when the wind forcing is turned off (Run W2). The summertime VET volume is 8.88 km^3 in the Base Run (Table 1). In the Runs W1 and W2, these volumes are 0.69 and 16.61 km^3, respectively. The corresponding hypoxic volume for each case shows similar variations and the values are close to the VET volume (Table 1). In order to quantify the relative effects of the

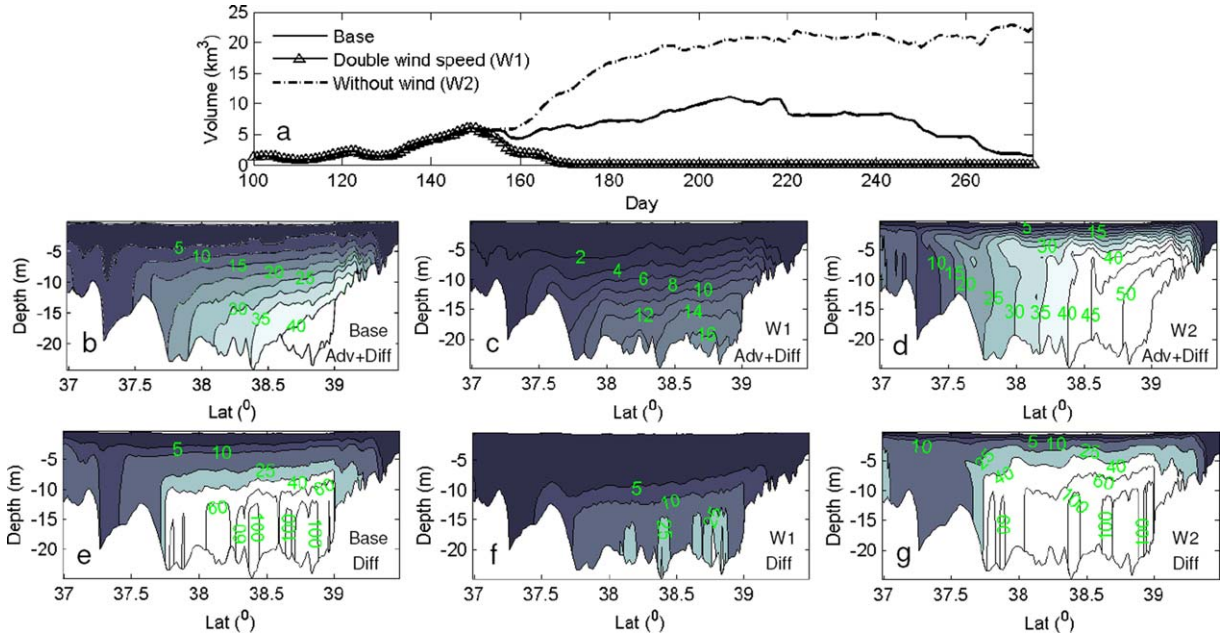

Figure 7. (a) Time series of volume of water mass with VET >23 days for the Base Run and two sensitivity runs (W1: double the wind speed after Day 150; W2: turn off wind after Day 150); (b–d) vertical profile of summertime (July–August) vertical exchange time for the Base Run, W1 and W2, respectively; (e–g) same as Figures 7b–7d but for the vertical exchange time caused by diffusion process only. Profiles are plotted along the deep channel of the Bay.

local vertical diffusion process and lateral circulation in changing the VET, the VET only induced by the vertical diffusion process (V-VET hereafter) is computed by turning off the advection terms in equations (2) and (3), respectively. The summertime profiles of VET along the deep channel of the Bay are shown in Figures 7b–7g. By comparing with the cases with complete hydrodynamic processes (Figures 7b–7d), the results indicate that the VET below the pycnocline increases greatly when the vertical exchange is only driven by the vertical diffusion process (Figures 7e–7g). In the Base Run, the V-VET is larger than 40 days below 10 m in the middle and upper-Bay and the bottom V-VET can reach 100 days (Figure 7e). When both advection and diffusion processes are included, it only results in a very small portion of the Bay with VET >40 days (Figure 7b). In the case with wind speed doubled (Run W1), both the VET and the V-VET decreases greatly and its pattern is totally changed (Figures 7c and 7f). The intensified wind forcing results in the destratified water column (figure not shown). Even the vertical diffusion process can induce very active vertical exchange and the area with V-VET >25 days almost disappeared (Figure 7f). When the advection process is included, the bottom layer VET is largely less than 16 days (Figure 7c). On the contrary, in the case with wind turned off (Run W2), the surface mixed layer that usually appeared in the estuary is replaced by the highly stratified water and the pycnocline is elevated above 6 m (figure not shown). As a result, the vertical exchange is severely suppressed (Figures 7d and 7g). Note that, in this case, the water column is less stratified in the bottom layers (figure not shown) so the isolines of the VET and V-VET are mainly perpendicular to the bottom in the bottom layers. Without advection process, it will take about 60 days for water mass being transported from water surface to the 10 m depth (Figure 7g). All this information indicates that, compared with vertical diffusion, the advection is the dominant process to facilitate vertical exchange in the water column and, thereby, to replenish bottom DO.

[25] Although the wind used in the sensitivity experiment is artificial, these results show that high-speed winds can play an important role in replenishing bottom DO. Figure 8 presents the wind speed at Solomons Island superimposed by the VET averaged in the section across the mid-Bay (see Figure 1b for the location). It can be seen that the occurrence of high-speed wind (especially with wind speed >10 m s^{-1}) is usually coincident with the occurrence of a sharp decrease in the VET. The surface DO can be transported to the bottom layers within a short time under such a high-speed wind forcing (Figure 7c). The pycnocline usually works as a barrier layer of vertical transportation of DO. The pycnocline can be destroyed (which facilitates vertical diffusion) or tilted (which intensifies lateral

Table 1. VET Volume (Defined by the Volume of Water Mass With Vertical Exchange Time >23 days) and Hypoxic Volume (DO >2 mg L^{-1}) for the Base Run, the Run with Doubled Wind Speed After Day 150 (W1), and the Run With Wind Turned Off (W2)

	VET Volume (km^3)	Hypoxic Volume (km^3)
Base Run	8.88	8.35
Double wind speed (W1)	0.69	0.65
Without wind (W2)	16.61	14.72

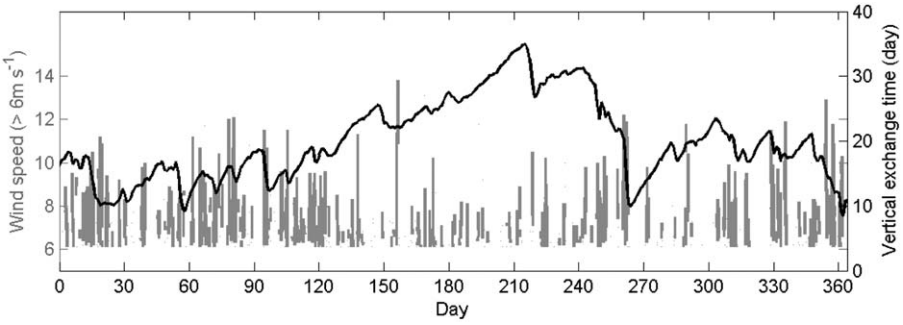

Figure 8. Wind speed (>6 m) at Solomons Island superimposed by the vertical exchange time averaged in the section across the mid-Bay (marked in Figure 1b) for water mass with depth greater than 8 m.

circulation) under such wind events. Either process can increase the vertical exchange of the estuary. Therefore, the passage of a synoptic wind event can result in a sharp decrease of the VET and fast replenishment of DO.

5.2. Effect of River Discharge

[26] Previous studies show that the spring river discharge has a profound impact on the summer water column stratification in the Chesapeake Bay [*Boicourt*, 1992; *Hagy*, 2002]. A strong stratification will affect the transport of surface high DO water across the pycnocline. It is interesting to investigate the effect of river discharge on the VET. We conducted three sensitivity experiments, R1 (using constant annual mean river discharge after Day 60), R2 (using half of the constant annual mean river discharge after Day 60), and R3 (reducing the observed river discharge by 70%) to investigate the responses of VET. Other forcings are the same as those in the Base Run.

[27] The high river discharge pulses appeared after Day 60 in 2004 (Figure 9a). By replacing the spring river discharge pulses with constant annual mean flow, the freshwater pulse was removed. Figure 9b presents the time series of VET volume (volume of water mass with VET >23 days). It can be seen that there are only minor changes in the VET volume although the model was forced by the mean flow (Run R1). When half of the constant annual mean river discharge was used (Run R2), the difference of the VET volume only occurs in the late spring until early summer. The difference tends to diminish after June. Several studies suggested that the January-to-May averaged Susquehanna River discharge is closely correlated with the hypoxic volume in the Bay, due to both freshwater input and nutrient loadings [e.g., *Hagy et al*., 2002; *Murphy et al*., 2011]. The January-to-May averaged river discharge in 2004 was 1865.70 $m^3 s^{-1}$ for the Base Run. For the sensitivity experiments R1 and R2, the discharges were 1727.59 and 1075.98 $m^3 s^{-1}$, respectively. After removing the spring river discharge pulses after Day 60, the major changes of stratification appear from Day 90 to Day 160 compared to the Base Run, and the changes of R1 are less than those of R2 (figure not shown). However, the summertime stratification only experienced minor changes. It appears that the effect of springtime river discharge pulses on the summertime VET volume decreases after several mouths of adjustment.

[28] Although the sensitivity experiments R1 and R2 removed freshwater discharge pulses, the initial status of the estuary was very stratified. To investigate further the

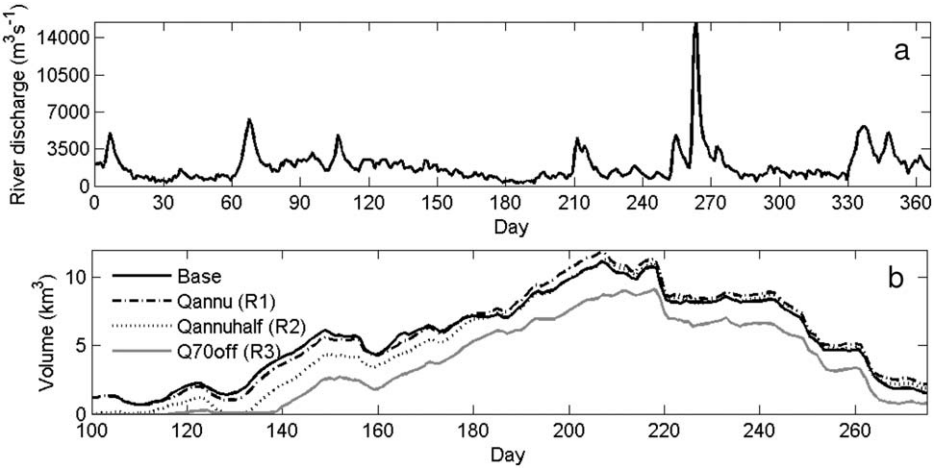

Figure 9. (a) Susquehanna River discharge ($m^3 s^{-1}$) in 2004; (b) time series of volume of water mass with vertical exchange time >23 days for the Base Run and three sensitivity runs (R1: constant annual mean river discharge after Day 60; R2: constant half of the annual mean river discharge after Day 60; R3: reduce the observed river discharge by 70%).

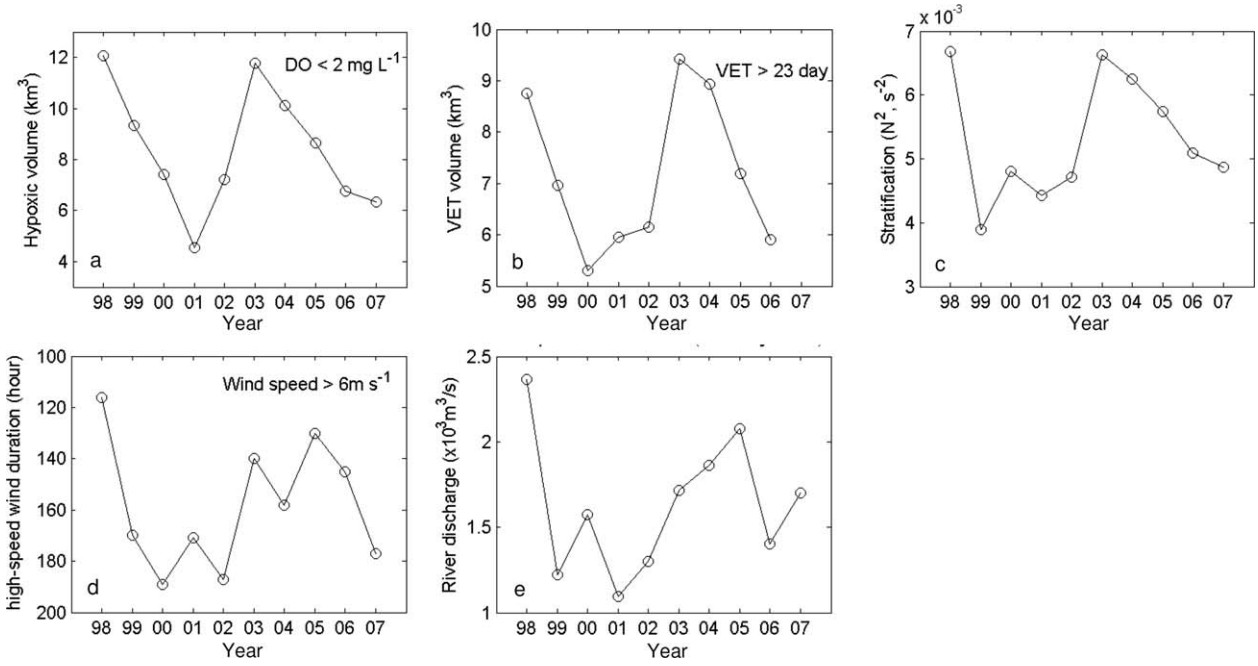

Figure 10. Time series of (a) observed summertime hypoxic volume (<2 mg L^{-1}) for Chesapeake Bay; (b) modeled summertime VET volume (volume of water mass with vertical exchange time >23 days); (c) stratification (N2) averaged from May to July; (d) summertime high-speed wind (>6 m s^{-1}) duration; (e) January-to-May averaged Susquehanna River discharge.

influence of river discharge, an experiment was conducted by reducing the observed river discharge by 70% (R3). The mean discharges from January to May from the Susquehanna River were 1865.70 and 559.71 m^3 s^{-1}, respectively, in the Base Run and Run R3. In this case, the time series of the VET volume of Run R3 shows a remarkable decrease. When the averaged Susquehanna River discharge from January to May was reduced by 70%, the VET volume was reduced by 20%. This result indicates that the VET volume is sensitive to the total amount of river discharge. A large VET volume can be expected in the wet year, which is consistent with findings from previous studies indicating that the wet year usually has a large hypoxic volume [e.g., *Murphy et al*., 2011].

5.3. Interpretation of Interannual Variation

[29] The time series of observed summertime hypoxic volume (DO <2 mg L^{-1}) is shown in Figure 10a. The data are obtained from the Chesapeake Bay Water Quality Monitoring Program (http://www.chesapeakebay.net/data_waterquality.aspx). From 1998 to 2007, large interannual variations of hypoxic volume can be observed. Large hypoxic volumes were observed in 1998 and 2003 while small hypoxic volumes were observed in 2001, 2006, and 2007. Using the HEM-3D model, we computed the VET in the Bay from 1998 to 2006. The VET volume (volume of water mass with VET >23 days) was calculated. The time series of the summertime VET volume is presented in Figure 10b. Compared with the time series of the hypoxic volume, a similar pattern of interannual variations can be found in the VET volume. These results indicate that the VET is highly correlated with the hypoxia in both the seasonal feature and the interannual variations (also see Figure 11). Corresponding to the high hypoxic volumes in 1998 and 2003, the VET volumes are also large in these 2 years. Figure 10c presents the time series of stratification (N^2) averaged from May to July by using the model results. It is obvious that the year with stronger stratification has larger hypoxic volume and larger VET volume. Although the VET volume generally shows similar interannual variations to the hypoxic volume, we notice that the smallest VET volume occurred in 2000 but the smallest hypoxic volume occurred in 2001, and the weakest stratification occurred in

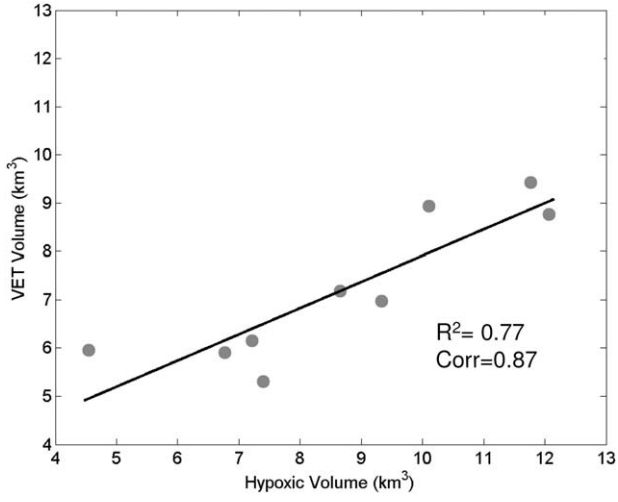

Figure 11. Scatter diagram of hypoxic volume and VET volume shown in Figures 10a and 10b, respectively. Solid line is the linear fit. R2 is 0.77. The correlation coefficient is 0.87 with 95% confidence level.

1999. Such discrepancy mainly occurs during the year with relatively weaker stratification. Both the variations of wind and river discharge can contribute to the interannual variations of stratification, VET volume, and hypoxic volume. We further analyzed the summertime high-speed wind duration from 1998 to 2007 by using the wind data observed at the Solomons Island station. Winds with magnitudes larger than 6 m s^{-1} were considered as high-speed winds. The duration of high-speed winds was calculated as the number of hours when a speed of 6 m s^{-1} was exceeded, irrespective of the direction of the wind and the number of consecutive hours when this limit was exceeded. The resulting time series is shown in Figure 10d. It should be noted that Figure 10d has a reversed *y* axis. A longer duration of high-speed wind should result in smaller VET and hypoxic volume as the ventilation caused by the high-speed wind events can greatly reduce the VET. The year 1998 has the shortest duration of high-speed wind. A longer duration of high-speed wind can be observed from 1999 to 2002. The time series of January-to-May averaged Susquehanna River discharge (Figure 10e) shows that flow in years 1999–2002 is relatively lower than other years. Although year 2001 has relatively lower river discharge than other years, the duration of high-speed wind in this year is shorter than those for 2000 and 2002. The resulting VET volume is the competition between buoyancy input by river discharge and the momentum input by wind forcing. When the ventilation caused by the high-speed wind events overcomes the suppression caused by strong stratification, the resulting VET volume will be small, and vice versa.

[30] The regression of summertime hypoxic volume and VET volume indicates that interannual variations of VET volume can be used to predict the variations of hypoxic volume (Figure 11). Their correlation coefficient is 0.87 (with 95% confidence level). The interannual variations of N^2 are frequently used to explain the variations of hypoxic volume [e.g., *Murphy et al*., 2011], which can be estimated based on the observed salinity data. The advantage of using VET is that it provides a common currency, which can be directly compared to the timescale of the oxygen consumption. It also provides information for the region where low DO can occur. Based on the conceptual model and regression results, the VET can be conveniently used to estimate bottom DO in the Bay if we know the oxygen consumption rate. For example, when the oxygen consumption rate is 0.30 g O_2 m^{-3} d^{-2} and the bottom VET is 20 days, it can be expected that the bottom layer DO will be consumed by 6 mg L^{-1} on average. The DO condition will be changed as the DO consumption rate changes. It can be expected that the critical VET value (>23 days) for the development of hypoxia (<2 mg L^{-1}) in the Bay may vary around 23 days when the total DO consumption rate changes. Although the summertime VET volume is significantly correlated with the hypoxic volume, it cannot catch all the variations as it can only explain the contribution of physical processes which regulates the DO replenishment. The deviation is due to biochemical processes related to nitrogen loading [*Murphy et al.*, 2011; *Scully*, 2010b]. For example, the year 2001 has the lowest hypoxic volume, but its VET volume is not the lowest (Figures 10a and 10b). The differences between hypoxic volume and the VET volume in these years may result from the difference of biochemical DO consumption.

6. Conclusion

[31] The vertical exchange time is introduced and linked with the hypoxia in the Chesapeake Bay. The VET is a suitable parameter for evaluating the variations of bottom DO concentration in both seasonal and interannual timescales. The VET is negatively correlated with DO concentration. The bottom DO will be less than 2 mg L^{-1} when the VET is greater than 23 days in summer for a total oxygen consumption rate of approximately 0.3 g O_2 m^{-3} d^{-1}. It can be expected that the critical VET value may vary around 23 days when the total DO consumption rate changes. The VET can be conveniently used to estimate bottom DO in the Bay if we know the oxygen consumption rate. The volume of water mass with VET >23 days is correlated with the hypoxic volume (DO <2 mg L^{-1}) in the Chesapeake Bay. The results indicate that the VET volume can account for 77% of variations of hypoxic volume in the main Bay based on model simulation results. The VET cannot explain all the DO variations as it can only account for the contribution of physical processes that regulate the DO replenishment. The deviation is due to the biochemical processes that cannot be reflected by the VET.

[32] The seasonal feature and synoptic scale variations shown in the DO field can be well interpreted by the variations of the VET. The effects of wind forcing and river discharge on VET are examined. Sensitivity experiments indicate that the short-term vertical exchange process is highly controlled by the wind forcing. The high-speed wind duration is found to be highly correlated with the ventilation of bottom waters in the Bay. The occurrence of high-speed wind is usually coincident with the occurrence of a sharp decrease in the VET. Diagnostic analyses indicate that the advection process is the dominant process to replenish bottom DO. By removing the spring river discharge pulses, the summertime VET has only very minor changes. The VET is sensitive to the total amount of river discharge. The high VET volume can be expected in a wet year.

[33] **Acknowledgments.** This work was supported by NOAA Coastal Modeling Testbed project and the South China University of Technology 985 project teaching staff construction founding. This paper is Contribution No. 3313 of the Virginia Institute of Marine Science, The College of William and Mary. We thank Mac Sisson at VIMS for his help in editing the manuscript. This work was performed using computational facilities at the College of William and Mary which were enabled by grants from Sun Microsystems, the National Science Foundation, and Virginia's Commonwealth Technology Research Fund.

References

Boicourt, W. C. (1992), Influences of circulation processes on dissolved oxygen in the Chesapeake Bay, in *Oxygen Dynamics in the Chesapeake Bay. A Synthesis of Recent Research Maryland Sea Grant College*, edited by D. E. Smith, M. Leffler, and G. Mackiernan, pp. 7–59, College Park, Md.

Boynton, W. R., and W. M. Kemp (1985), Regeneration and oxygen consumption by sediments along an estuarine salinity gradient, *Mar. Ecol. Prog. Ser.*, *23*, 45–55.

Cerco, C. F. (1995), Simulation of long-term trends in Chesapeake Bay eutrophication, *J. Environ. Eng.*, *121*(4), 298–310.

Cowan, J. L. W., and W. R. Boynton (1996), Sediment-water oxygen and nutrient exchanges along the longitudinal axis of Chesapeake Bay: Seasonal patterns, controlling factors and ecological significance, *Estuaries*, *19*(3), 562–580.

Deleersnijder, E., J. Campin, and E. Delhez (2001), The concept of age in marine modeling. I: Theory and preliminary model results, *J. Mar. Syst.*, *28*, 229–267.

Delhez, E. J. M., A. W. Heemink, and E. Deleersnijder (2004), Residence time in a semi-enclosed domain from the solution of an adjoint problem, *Estuarine Coastal Shelf Sci.*, *61*, 691–702.

England, J. H. (1995), The age of water and ventilation timescales in a global ocean model, *J. Phys. Oceanogr.*, *25*, 2756–2777.

Galperin, B., L. H. Kantha, S. Hassis, and A. Rosati (1988), A quasi-equilibrium turbulent energy model for geophysical flows, *J. Atmos. Sci.*, *45*, 55–62.

Gustafsson, K. E., and J. Bendtsen (2007), Elucidating the dynamics and mixing agents of a shallow fjord through age tracer modeling, *Estuarine Coastal Shelf Sci.*, *74*(4), 641–654.

Hagy, J. D. (2002), Eutrophication, hypoxia and trophic transfer efficiency in Chesapeake Bay, PhD dissertation, Univ. of Maryland, College Park, Md.

Hagy, J. D., W. R. Boynton, C. W. Keefe, and K. V. Wood (2004), Hypoxia in Chesapeake Bay, 1950–2001: Long-term change in relation to nutrient loading and river flow, *Estuaries*, *27*, 634–658.

Hamrick, J. M., and T. S. Wu (1997), Computational design and optimization of the EFDC/HEM3D surface water hydrodynamic and eutrophication models, in *Next Generation Environmental Models and Computational Methods*, edited by G. Delich and M. F. Wheeler, pp. 143–161, Soc. for Ind. and Appl. Math., Philadelphia, Pa.

Hohmann, R., M. Hofer, R. Kipfer, F. Peeters, D. M. Imboden, H. Baur, and M. N. Shimaraev (1998), Distribution of helium and tritium in Lake Baikal, *J. Geophys. Res.*, *103*, 12,823–12,838.

Hong, B., and J. Shen (2012), Responses of estuarine salinity and transport processes to potential future sea-level rise in the Chesapeake Bay, *Estuarine Coastal Shelf Sci. 104–105*, 33–45.

Jenkins, W. J. (1987), 3H and 3He in the beta triangle: Observations of gyre ventilation and oxygen utilization rates, *J. Phys. Oceanogr.*, *17*, 763–783.

Kuo, A. Y., and B. J. Neilson (1987), Hypoxia and salinity in Virginia Estuaries, *Estuaries*, *10*(4), 277–283.

Li, Y., and M. Li (2011), Effects of winds on stratification and circulation in a partially mixed estuary, *J. Geophys. Res.*, *116*, C12012, doi: 10.1029/2010JC006893.

Lucas, L. V., J. K. Thompson, and L. R. Brown (2009), Why are diverse relationship observed between phytoplankton biomass and transport time?, *Limnol. Oceanogr.*, *54*(1), 381–390.

MacCready, P. (2004), Toward a unified theory of tidally-averaged estuarine salinity structure, *Estuaries*, *27*(4), 561–570.

Mellor, G. L., and T. Yamada (1982), Development of a turbulence closure model for geophysical fluid problems, *Rev. Geophys. Space Phys.*, *20*, 851–875.

Murphy, R., W. Kemp, and W. Ball (2011), Long-term trends in Chesapeake Bay seasonal hypoxia, stratification, and nutrient loading, *Estuaries Coasts*, *34*, 1293–1309, doi:10.1007/s12237-011-9413-7.

Officer, C. B. (1976), *Physical Oceanography of Estuaries (and Associated Coastal Waters)*, John Wiley, New York.

Park, K., A. Y. Kuo, J. Shen, J. M. Hamrick (1995), A three-dimensional hydrodynamic eutrophication model (HEM-3D): Description of water quality and sediment process submodels, *Spec. Rep. in Appl. Mar. Sci. and Ocean Eng. 327*, 102 pp., Virginia Inst. of Mar. Sci., Gloucester Point, Va.

Pritchard, D. W. (1952), Salinity distribution and circulation in the Chesapeake Bay estuaries system, *J. Mar. Res.*, *11*, 106–23.

Rabalais, N. N., R. E. Turner, and D. Scavia (2002), Beyond science into policy: Gulf of Mexico hypoxia and the Mississippi River, *Bioscience*, *52*, 129–142.

Sarmiento, J. L., G. Thiele, R. M. Key, and W. S. Moore (1990), Oxygen and nitrate new production and remineralization in the North Atlantic subtropical gyre, *J. Geophys. Res.*, *95*, 18,303–18,315.

Schlosser, P., J. L. Bullister, R. A. Fine, W. J. Jenkins, R. Key, J. Lupton, W. Roether, and W. M. Smethie, Jr. (2001), Transformation and age of water masses, in *Ocean Circulation and Climate: Observing and Modelling the Global Ocean*, edited by G. Siedler, J. Church, and J. Gould, pp. 431–452, Academic Press, New York.

Scully, M. E. (2010a), Wind modulation of dissolved oxygen in Chesapeake Bay, *Estuaries Coasts*, *33*, 1164–1175.

Scully, M. E. (2010b), The Importance of climate variability to wind-driven modulation of hypoxia in Chesapeake Bay, *J. Phys. Oceanogr.*, *40*, 1435–1440.

Seliger, H. H., and J. A. Boggs (1988), Long term pattern of anoxia in the Chesapeake Bay, in *Understanding the Estuary: Advances in Chesapeake Bay Research*, edited by M. Lynch and E. C. Krome, pp. 570–583, Chesapeake Res. Consortium Publ. 129, Solomons, Md.

Shen, J., and L. Haas (2004), Calculating age and residence time in the tidal York River using three-dimensional model experiments, *Estuarine Coastal Shelf Sci.*, *61*, 449–461.

Shen, J., B. Hong, and A. Y. Kuo (2013), Using timescales to interpret dissolved oxygen distributions in the bottom waters of Chesapeake Bay, Limno, *Oceanogr.*, *58*(6), doi:10.4319/lo.2013.58-06.0000.

The Chesapeake Bay Foundation (2008), The Chesapeake Bay's Dead Zone. [Available at http://www.cbf.org/site/PageServer?pagename=resources_facts_deadzone.]

Thomann, R. V., and J. A. Mueller (1987), *Principles of Surface Water Quality Modeling and Control*, 644 pp., Harper and Row, New York.

Waugh, D. W., T. M. Hall, and T. W. N. Haine (2003), Relationship among tracer ages, *J. Geophys. Res.*, *108*(5), 3138, doi:10.1029/2002JC001325.

Wilson, R. E., R. L. Swanson, and H. A. Crowley (2008), Perspectives on long-term variations in hypoxic conditions in western Long Island Sound, *J. Geophys. Res.*, *113*, C12011, doi:10.1029/2007JC004693.